

Measurement of the Inclusive Charmless Semileptonic Partial Branching Fraction of B Mesons and Determination of $|V_{ub}|$ using the Full Reconstruction Tag

I. Bizjak,¹² K. Abe,⁷ K. Abe,⁴¹ H. Aihara,⁴³ Y. Asano,⁴⁷ S. Bahinipati,⁴ A. M. Bakich,³⁸ Y. Ban,³² E. Barberio,¹⁹ M. Barbero,⁶ A. Bay,¹⁶ U. Bitenc,¹² S. Blyth,²⁴ A. Bondar,¹ A. Bozek,²⁵ M. Bračko,^{7,18,12} J. Brodzicka,²⁵ T. E. Browder,⁶ Y. Chao,²⁴ A. Chen,²² W. T. Chen,²² B. G. Cheon,³ R. Chistov,¹¹ S.-K. Choi,⁵ Y. Choi,³⁷ Y. K. Choi,³⁷ A. Chuvikov,³³ S. Cole,³⁸ J. Dalseno,¹⁹ M. Danilov,¹¹ M. Dash,⁴⁸ L. Y. Dong,⁹ A. Drutskoy,⁴ S. Eidelman,¹ Y. Enari,²⁰ F. Fang,⁶ S. Fratina,¹² N. Gabyshev,¹ A. Garmash,³³ T. Gershon,⁷ G. Gokhroo,³⁹ B. Golob,^{17,12} A. Gorišek,¹² J. Haba,⁷ T. Hara,³⁰ H. Hayashii,²¹ M. Hazumi,⁷ L. Hinz,¹⁶ T. Hokuue,²⁰ Y. Hoshi,⁴¹ S. Hou,²² W.-S. Hou,²⁴ T. Iijima,²⁰ A. Imoto,²¹ K. Inami,²⁰ A. Ishikawa,⁷ R. Itoh,⁷ M. Iwasaki,⁴³ Y. Iwasaki,⁷ J. H. Kang,⁴⁹ J. S. Kang,¹⁴ P. Kapusta,²⁵ N. Katayama,⁷ H. Kawai,² T. Kawasaki,²⁷ H. R. Khan,⁴⁴ H. Kichimi,⁷ H. J. Kim,¹⁵ S. M. Kim,³⁷ K. Kinoshita,⁴ S. Korpar,^{18,12} P. Križan,^{17,12} P. Krokovny,¹ R. Kulasiri,⁴ S. Kumar,³¹ C. C. Kuo,²² A. Kuzmin,¹ Y.-J. Kwon,⁴⁹ G. Leder,¹⁰ S. E. Lee,³⁶ T. Lesiak,²⁵ J. Li,³⁵ A. Limosani,⁷ S.-W. Lin,²⁴ D. Liventsev,¹¹ J. MacNaughton,¹⁰ G. Majumder,³⁹ F. Mandl,¹⁰ T. Matsumoto,⁴⁵ A. Matyja,²⁵ Y. Mikami,⁴² W. Mitaroff,¹⁰ K. Miyabayashi,²¹ H. Miyake,³⁰ H. Miyata,²⁷ R. Mizuk,¹¹ T. Nagamine,⁴² Y. Nagasaka,⁸ I. Nakamura,⁷ E. Nakano,²⁹ M. Nakao,⁷ Z. Natkaniec,²⁵ S. Nishida,⁷ O. Nitoh,⁴⁶ T. Nozaki,⁷ S. Ogawa,⁴⁰ T. Ohshima,²⁰ T. Okabe,²⁰ S. Okuno,¹³ S. L. Olsen,⁶ Y. Onuki,²⁷ W. Ostrowicz,²⁵ P. Pakhlov,¹¹ H. Park,¹⁵ N. Parslow,³⁸ L. S. Peak,³⁸ R. Pestotnik,¹² L. E. Piilonen,⁴⁸ M. Rozanska,²⁵ H. Sagawa,⁷ Y. Sakai,⁷ N. Sato,²⁰ T. Schietinger,¹⁶ O. Schneider,¹⁶ P. Schönmeier,⁴² C. Schwanda,¹⁰ K. Senyo,²⁰ M. E. Sevior,¹⁹ H. Shibuya,⁴⁰ B. Shwartz,¹ V. Sidorov,¹ A. Somov,⁴ N. Soni,³¹ R. Stamen,⁷ S. Stanič,²⁸ M. Starič,¹² T. Sumiyoshi,⁴⁵ S. Suzuki,³⁴ S. Y. Suzuki,⁷ O. Tajima,⁷ F. Takasaki,⁷ K. Tamai,⁷ N. Tamura,²⁷ M. Tanaka,⁷ Y. Teramoto,²⁹ X. C. Tian,³² T. Tsuboyama,⁷ T. Tsukamoto,⁷ S. Uehara,⁷ T. Uglov,¹¹ K. Ueno,²⁴ S. Uno,⁷ P. Urquijo,¹⁹ G. Varner,⁶ K. E. Varvell,³⁸ S. Villa,¹⁶ C. C. Wang,²⁴ C. H. Wang,²³ Y. Watanabe,⁴⁴ Q. L. Xie,⁹ B. D. Yabsley,⁴⁸ A. Yamaguchi,⁴² Y. Yamashita,²⁶ M. Yamauchi,⁷ Heyoung Yang,³⁶ L. M. Zhang,³⁵ Z. P. Zhang,³⁵ V. Zhilich,¹ and D. Žontar^{17,12}

(The Belle Collaboration)

¹Budker Institute of Nuclear Physics, Novosibirsk

²Chiba University, Chiba

³Chonnam National University, Kwangju

⁴University of Cincinnati, Cincinnati, Ohio 45221

⁵Gyeongsang National University, Chinju

⁶University of Hawaii, Honolulu, Hawaii 96822

⁷High Energy Accelerator Research Organization (KEK), Tsukuba

⁸Hiroshima Institute of Technology, Hiroshima

⁹Institute of High Energy Physics, Chinese Academy of Sciences, Beijing

¹⁰Institute of High Energy Physics, Vienna

¹¹Institute for Theoretical and Experimental Physics, Moscow

¹²J. Stefan Institute, Ljubljana

¹³Kanagawa University, Yokohama

¹⁴Korea University, Seoul

¹⁵Kyungpook National University, Taegu

¹⁶Swiss Federal Institute of Technology of Lausanne, EPFL, Lausanne

¹⁷University of Ljubljana, Ljubljana

¹⁸University of Maribor, Maribor

¹⁹University of Melbourne, Victoria

²⁰Nagoya University, Nagoya

²¹Nara Women's University, Nara

²²National Central University, Chung-li

²³National United University, Miao Li

²⁴Department of Physics, National Taiwan University, Taipei

²⁵H. Niewodniczanski Institute of Nuclear Physics, Krakow

²⁶Nippon Dental University, Niigata

²⁷Niigata University, Niigata

²⁸Nova Gorica Polytechnic, Nova Gorica

²⁹Osaka City University, Osaka

³⁰Osaka University, Osaka

³¹Panjab University, Chandigarh

³²Peking University, Beijing
³³Princeton University, Princeton, New Jersey 08544
³⁴Saga University, Saga
³⁵University of Science and Technology of China, Hefei
³⁶Seoul National University, Seoul
³⁷Sungkyunkwan University, Suwon
³⁸University of Sydney, Sydney NSW
³⁹Tata Institute of Fundamental Research, Bombay
⁴⁰Toho University, Funabashi
⁴¹Tohoku Gakuin University, Tagajo
⁴²Tohoku University, Sendai
⁴³Department of Physics, University of Tokyo, Tokyo
⁴⁴Tokyo Institute of Technology, Tokyo
⁴⁵Tokyo Metropolitan University, Tokyo
⁴⁶Tokyo University of Agriculture and Technology, Tokyo
⁴⁷University of Tsukuba, Tsukuba
⁴⁸Virginia Polytechnic Institute and State University, Blacksburg, Virginia 24061
⁴⁹Yonsei University, Seoul

We present a measurement of the inclusive charmless semileptonic partial branching fraction of the B meson, based on 253 fb^{-1} of data collected by the Belle detector at the KEKB e^+e^- asymmetric collider. Events are tagged by fully reconstructing one of the B mesons, produced in pairs from $\Upsilon(4S)$. The signal for $b \rightarrow u$ semileptonic decay is distinguished from the $b \rightarrow c$ semileptonic background using three kinematic variables: the hadronic mass M_X , the leptonic invariant mass squared q^2 and the variable $P_+ \equiv E_X - |\vec{p}_X|$. We measure partial branching fractions $\Delta\mathcal{B}(B \rightarrow X_u \ell \nu)$ for events with the prompt-lepton momentum $p_\ell^* \geq 1 \text{ GeV}/c$, in the three kinematic regions $M_X < 1.7 \text{ GeV}/c^2$, $M_X < 1.7 \text{ GeV}/c^2$ combined with $q^2 > 8 \text{ GeV}^2/c^2$, and by $P_+ < 0.66 \text{ GeV}/c$. From these measurements, the magnitude of the Cabibbo-Kobayashi-Maskawa matrix element V_{ub} is derived.

PACS numbers: 12.15.Hh, 11.30.Er, 13.25.Hw

An accurate knowledge of the Cabibbo-Kobayashi-Maskawa matrix element $|V_{ub}|$ is crucial to test Standard Model predictions for CP violation. One of the best ways to determine $|V_{ub}|$ is to measure $\Delta\mathcal{B}(B \rightarrow X_u \ell \nu)$, the inclusive charmless semileptonic partial branching fraction of the B meson. Here we report a measurement of $\Delta\mathcal{B}(B \rightarrow X_u \ell \nu)$ with a sample of events where the hadronic decay mode of the tagging side B meson, B_{tag} , is fully reconstructed, while the semileptonic decay of the signal side B meson, B_{sig} , is identified by the presence of a high momentum electron or muon.

This method allows the construction of the invariant masses of the hadronic (M_X) and leptonic ($\sqrt{q^2}$) system in the semileptonic decay, and the variable $P_+ \equiv E_X - |\vec{p}_X|$, where E_X is the energy and $|\vec{p}_X|$ the magnitude of the three-momentum of the hadronic system. These inclusive kinematic variables can, according to recent theoretical studies [1, 2], be used to separate the $B \rightarrow X_u \ell \nu$ decays from the much more abundant $B \rightarrow X_c \ell \nu$ decays, while minimizing the uncertainty in the extrapolation to the full phase space of the decay. Three different kinematic regions are chosen for this analysis based on these three kinematic variables, and the experimental results are given in terms of partial branching fractions for each region. The corresponding values of $|V_{ub}|$ are extracted using recent theoretical calculations [2, 3] that include all the currently known contributions in a consistent frame-

work. A similar type of analysis was performed by the BaBar Collaboration, where only a cut on M_X was applied [4], and by Belle, where a requirement on M_X and q^2 was used [5]. The present analysis is the first one to use the variable P_+ to extract $|V_{ub}|$.

The data were collected with the Belle detector [6] at the asymmetric-energy KEKB storage ring [7]. The results presented in this paper are based on a 253 fb^{-1} sample recorded at the $\Upsilon(4S)$ resonance, which contains $275 \times 10^6 B\bar{B}$ pairs. An additional 28 fb^{-1} sample taken at a center-of-mass energy 60 MeV below the $\Upsilon(4S)$ resonance is used to subtract the background from $e^+e^- \rightarrow q\bar{q}$ ($q = u, d, s, c$).

Monte Carlo (MC) simulated events were used to determine efficiencies as well as signal and background distributions. The detector simulation was based on GEANT [8]. To model $B \rightarrow X_u \ell \nu$ we use the EvtGen generator [9] with various models, where X_u is π or ρ [10], an excited X_u state [11], or a non-resonant multiparticle final state [12]. The $B \rightarrow X_c \ell \nu$ transitions are simulated according to the QQ generator [13]. For the two dominant contributions, $D^* \ell \nu$ and $D \ell \nu$, we use an HQET-based parametrization of form factors [14] and ISGW2 model [11], respectively. The motion of the b quark inside the B meson is implemented with the introduction of a shape function [12, 15] that describes the b quark momentum distribution inside the B meson.

The B_{tag} candidates are reconstructed in the modes $B \rightarrow D^{(*)}\pi/\rho/a_1/D_s^{(*)}$, $\bar{D}^0 \rightarrow K^+\pi^-$, $K^+\pi^-\pi^0$, $K^+\pi^+\pi^-\pi^-$, $K_S^0\pi^0$, $K_S^0\pi^+\pi^-$, $K_S^0\pi^+\pi^-\pi^0$ and K^+K^- , $D^- \rightarrow K^+\pi^-\pi^-$, $K^+\pi^-\pi^-\pi^0$, $K_S^0\pi^-$, $K_S^0\pi^-\pi^0$, $K_S^0\pi^-\pi^-\pi^+$ and $K^+K^-\pi^-$, and $D_s^+ \rightarrow K_S^0K^+$ and $K^+K^-\pi^+$. \bar{D}^* mesons are reconstructed by combining a \bar{D} candidate and a soft pion or photon. (Inclusion of charge conjugate decays is implied throughout this paper.) The selection of B_{tag} candidates is based on the beam-constrained mass, $M_{\text{bc}} = \sqrt{E_{\text{beam}}^{*2}/c^4 - p_B^{*2}/c^2}$, and the energy difference, $\Delta E = E_B^* - E_{\text{beam}}^*$. Here $E_{\text{beam}}^* = \sqrt{s}/2 \simeq 5.290 \text{ GeV}$ is the beam energy in the e^+e^- center-of-mass system (cms), and p_B^* and E_B^* are the cms momentum and energy of the reconstructed B meson. (Throughout this paper the variables calculated in the cms are denoted with an asterisk.)

The combinatorial background from jet-like $e^+e^- \rightarrow q\bar{q}$ processes is suppressed by an event topology requirement based on the normalized second Fox-Wolfram moment $R_2 < 0.5$ [16], and for some modes also by $|\cos \theta_{\text{thrust}}^*| < 0.8$, where θ_{thrust}^* is the angle between the thrust axis of the B_{tag} candidate and that of the rest of the event. To minimize the fraction of events with incorrect separation of tag and signal sides while maintaining high signal efficiency, a loose selection requirement of $M_{\text{bc}} \geq 5.22 \text{ GeV}/c^2$ and $-0.2 < \Delta E < 0.05 \text{ GeV}$ is made. If an event has multiple B_{tag} candidates, we choose the one having the smallest χ^2 based on ΔE , the D candidate mass, and the $D^* - D$ mass difference if applicable.

For events tagged by fully reconstructed B_{tag} candidates, we search for electrons or muons from semileptonic decays of B_{sig} . We require a lepton with momentum p_ℓ^* exceeding $1 \text{ GeV}/c$ in the laboratory polar angular region of $26^\circ \leq \theta \leq 140^\circ$. Leptons from J/ψ decay, photon conversion in the material of the detector, and π^0 decay are rejected based on the invariant mass they form in combination with an oppositely charged lepton and for electron candidates also with an additional photon. When the B_{tag} candidate is charged, we also require the lepton charge to be consistent with that from prompt semileptonic decay. The signal yield is obtained by fitting the M_{bc} distribution to the sum of an empirical parametrization of the combinatorial background shape [17] plus a signal shape [18] that peaks at the B mass and taking the part of the signal that lies in the “signal region,” $M_{\text{bc}} \geq 5.27 \text{ GeV}/c^2$, as shown in Fig. 1(a). The cutoff for M_{bc} reduces the uncertainty from the incorrect assignment of tag and signal sides in signal events.

The $B \rightarrow X_u \ell \nu$ signal events are selected by removing poorly measured soft charged tracks and imposing several additional requirements to reject poorly reconstructed events and suppress the $B \rightarrow X_c \ell \nu$ background. We require that the event contain exactly one lepton and have zero net charge and that the invariant mass squared

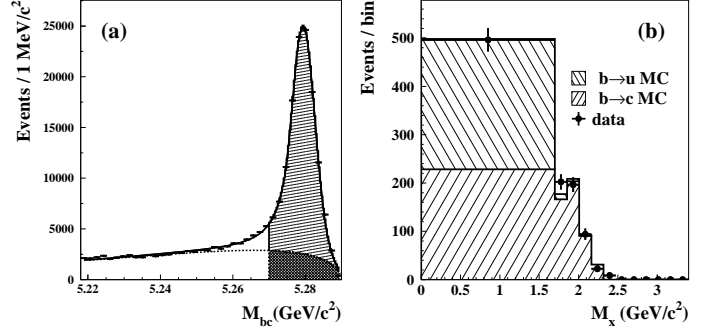


FIG. 1: (a) Distribution in M_{bc} (data) of B_{tag} candidates in events satisfying B_{sig} selection. (b) M_X distribution for events with $q^2 > 8 \text{ GeV}^2/c^2$, with fitted contributions of $B \rightarrow X_c \ell \nu$ and $B \rightarrow X_u \ell \nu$.

of the missing four-momentum $m_{\text{miss}}^2 \equiv (p_{\Upsilon(4S)} - p_{B_{\text{tag}}} - p_X - p_\ell)^2$ ($p_{\Upsilon(4S)}$, $p_{B_{\text{tag}}}$ and p_X are four-momenta of the $\Upsilon(4S)$, B_{tag} , and hadronic system (X), respectively) be consistent with zero. To suppress the $B \rightarrow X_c \ell \nu$ background, events with a K^\pm or K_S^0 candidate on the signal side are rejected (kaon veto). To reject events containing a K_L^0 , we require that the angle between the missing momentum and the direction of any K_L^0 candidate, reconstructed in the K_L^0 detector, be greater than 37 degrees. We also reject $B^0 \rightarrow D^{*+} \ell^- \bar{\nu}$ events by detecting the slow pion (π_s) from $D^{*+} \rightarrow D^0 \pi_s^+$ and deducing from its momentum the momentum of the D^{*+} . The missing mass squared $m_{\text{miss}(D^*)}^2 = (p_B - p_{D^*} - p_\ell)^2$ is calculated from the reconstructed quantities, and events with $m_{\text{miss}(D^*)}^2 > -3 \text{ GeV}^2/c^4$ are rejected.

Finally, the kinematic variables M_X and P_+ are calculated from the measured momenta of all charged tracks and energy deposits of all neutral clusters in the electromagnetic calorimeter that are not used in the B_{tag} reconstruction or for the lepton candidate. The four-momentum of the leptonic system is calculated as $q = p_{\Upsilon(4S)} - p_{B_{\text{tag}}} - p_X$. The distributions of events in M_X and P_+ are obtained by fitting the M_{bc} distribution, as described above, in bins of M_X and P_+ . Figures 1(b) and 2(a) show the resulting M_X and P_+ distributions. We define three kinematic signal regions for events where the prompt lepton has $p_\ell^* \geq 1 \text{ GeV}/c$: $P_+ < 0.66 \text{ GeV}/c$, $M_X < 1.7 \text{ GeV}/c^2$, and $M_X < 1.7 \text{ GeV}/c^2$ combined with $q^2 > 8 \text{ GeV}^2/c^2$. These three regions are denoted as P_+ , M_X and M_X/q^2 , respectively. To minimize the systematic effects of uncertainties in lepton selection and full reconstruction, the partial branching fraction is reported as a ratio, $\Delta \mathcal{B}(B \rightarrow X_u \ell \nu)/\mathcal{B}(B \rightarrow X \ell \nu)$, for all three signal regions, and obtained from the following equation:

$$\frac{\Delta \mathcal{B}(B \rightarrow X_u \ell \nu)}{\mathcal{B}(B \rightarrow X \ell \nu)} = \frac{N_{b \rightarrow u}^{\text{raw}}}{N_{\text{sl}}} \times \frac{F}{\varepsilon_{\text{sel}}^{b \rightarrow u}} \times \frac{\varepsilon_{\text{frec}}^{\text{sl}}}{\varepsilon_{\text{frec}}^{b \rightarrow u}} \times \frac{\varepsilon_\ell^{\text{sl}}}{\varepsilon_\ell^{b \rightarrow u}} \quad . \quad (1)$$

To extract the raw number of signal events, $N_{b \rightarrow u}^{\text{raw}}$, we

TABLE I: $N_{b \rightarrow u}^{\text{raw}}$, $\varepsilon_{\text{sel}}^{b \rightarrow u}$, F and $r_{b \rightarrow u}^{\text{sl}}$ for the three kinematic signal regions.

	$N_{b \rightarrow u}^{\text{raw}}$	$\varepsilon_{\text{sel}}^{b \rightarrow u}$	F	$r_{b \rightarrow u}^{\text{sl}}$
M_X/q^2	268 ± 27	26.5%	1.03	0.687 ± 0.014
M_X	404 ± 37	28.7%	1.07	0.700 ± 0.011
P_+	340 ± 32	25.5%	1.01	0.700 ± 0.012

TABLE II: Partial branching fraction with relative errors (in %) for the three kinematic signal regions.

	$\Delta \mathcal{B}(B \rightarrow X_u \ell \nu)$	stat	syst	$b \rightarrow u$	$b \rightarrow c$
M_X/q^2	8.41×10^{-4}	10.0	9.1	6.2	5.3
M_X	1.24×10^{-3}	9.1	7.4	6.1	2.2
P_+	1.10×10^{-3}	9.4	9.5	6.4	8.7

fit the M_X and P_+ distributions with MC-determined shapes for $B \rightarrow X_u \ell \nu$ and $B \rightarrow X_c \ell \nu$ and subtract the $B \rightarrow X_c \ell \nu$ contribution. The results for the M_X/q^2 and P_+ regions are shown in Figs. 1(b) and 2(a), respectively. MC simulation is used to estimate the conversion factor F of the observed number of events $N_{b \rightarrow u}^{\text{raw}}$ to the number of signal events produced in the region in question and observed anywhere, and to estimate the efficiency for these events, $\varepsilon_{\text{sel}}^{b \rightarrow u}$.

$N_{\text{sl}} = (9.14 \pm 0.05) \times 10^4$ is the number of events having at least one lepton with $p_\ell^* \geq 1 \text{ GeV}/c$, determined from a fit to the corresponding M_{bc} distribution (Fig. 1(a)), and corrected for the expected fraction of background events from non-semileptonic decays (14.0%), as estimated by MC simulation. The factor $\varepsilon_{\text{frec}}^{\text{sl}}/\varepsilon_{\text{frec}}^{b \rightarrow u}$ accounts for a possible difference in the B_{tag} reconstruction efficiency in the presence of a semileptonic or $B \rightarrow X_u \ell \nu$ decay; $\varepsilon_{\ell}^{\text{sl}}/\varepsilon_{\ell}^{b \rightarrow u}$ is the ratio of both lepton identification efficiencies and fractions of semileptonic decay leptons with $p_\ell^* \geq 1 \text{ GeV}/c$, in the whole kinematic phase space for semileptonic decays, and within the kinematic signal region for signal events. The product of efficiency ratios $r_{b \rightarrow u}^{\text{sl}} \equiv \varepsilon_{\text{frec}}^{\text{sl}}/\varepsilon_{\text{frec}}^{b \rightarrow u} \times \varepsilon_{\ell}^{\text{sl}}/\varepsilon_{\ell}^{b \rightarrow u}$ is obtained from MC simulation. Table I summarizes the results for $N_{b \rightarrow u}^{\text{raw}}$, $\varepsilon_{\text{sel}}^{b \rightarrow u}$, F and $r_{b \rightarrow u}^{\text{sl}}$ for all three signal regions, where the error in $N_{b \rightarrow u}^{\text{raw}}$ is statistical only. Inserting these values in Eq. 1, we obtain the three relative partial branching fractions. These are converted to partial branching fractions using the measured semileptonic branching fraction $\mathcal{B}(B \rightarrow X \ell \nu) = 0.1073 \pm 0.0028$ [19]. The results with relative errors are given in Table II.

We divide the experimental error into four categories: statistical, systematic, $b \rightarrow c$ and $b \rightarrow u$ MC modeling errors, and summarize them in Table II for the three partial branching fraction measurements. The two modeling errors include the uncertainty in signal event extraction, efficiency and unfolding factor determination due

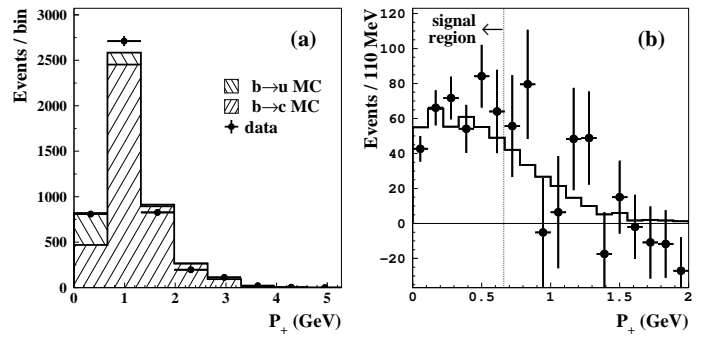


FIG. 2: (a) The P_+ distribution for the selected events, with fitted contributions from $B \rightarrow X_c \ell \nu$ and $B \rightarrow X_u \ell \nu$, (b) P_+ distribution (symbols with error bars) after subtracting $B \rightarrow X_c \ell \nu$, with fitted $B \rightarrow X_u \ell \nu$ contribution (histogram).

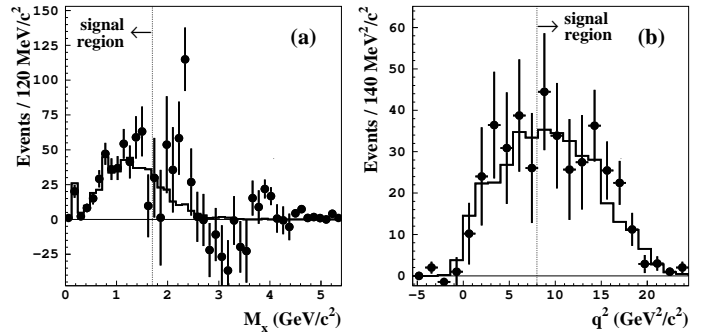


FIG. 3: Distributions in data after subtracting the $B \rightarrow X_c \ell \nu$ contribution (symbols with error bars), shown with contribution from $B \rightarrow X_u \ell \nu$ (MC, histogram), (a) in M_X (no q^2 requirement) and (b) in q^2 with $M_X < 1.7 \text{ GeV}/c^2$.

to the choice of specific theoretical models and values of the parameters used in our MC predictions. For signal $B \rightarrow X_u \ell \nu$ MC, the shape function parameters $\Lambda_{\text{SF}}^{\text{SF}} = (0.66 \pm 0.15) \text{ GeV}/c^2$ and $\lambda_1^{\text{SF}} = -(0.40 \pm 0.20) \text{ GeV}^2/c^2$ were varied within the stated limits, taking into account the negative correlation between them [20]. To take into account the uncertainty of the prediction in Ref. [12], we use a factor of two larger error for Λ^{SF} than was determined in Ref. [20]. For $B \rightarrow X_c \ell \nu$ MC, the uncertainty due to our limited knowledge of branching fractions is studied by varying the contributions of $D \ell \nu$ and $D^* \ell \nu$ and the relative fraction of narrow states D_1 and D_2^* that contribute to $D^{**} \ell \nu$ to estimate the modeling error of the D^{**} region. The uncertainty from form factor modeling in $D \ell \nu$ and $D^* \ell \nu$ was studied by varying the parameters $\rho_D^2 = 1.15 \pm 0.16$ and $\rho_A^2 = 1.56 \pm 0.13$ within their errors [19]. The validity of the $B \rightarrow X_c \ell \nu$ simulation was tested on a $B \rightarrow X_c \ell \nu$ enhanced control sample, where all selection requirements are applied but with the kaon veto reversed. The kinematic distributions of this control sample are accurately described by the simulation. Other sources of uncertainties, namely limited MC statis-

TABLE III: Obtained values of $|V_{ub}|$ with relative errors (in %) for the three kinematic signal regions. Shape function parameters used in the calculation are $m_b(\text{SF}) = 4.52 \text{ GeV}/c^2$ and $\mu_\pi^2(\text{SF}) = 0.27 \text{ GeV}^2/c^2$.

	$ V_{ub} \times 10^3$	stat	syst	$b \rightarrow u$	$b \rightarrow c$	SF	th.
M_X/q^2	4.93	5.0	4.4	3.1	2.7	9.3	$^{+5.0}_{-5.5}$
M_X	4.35	4.6	3.5	3.1	1.1	9.2	$^{+3.6}_{-3.9}$
P_+	4.56	4.7	4.6	3.2	4.4	10.2	$^{+3.4}_{-3.5}$

tics, extraction of $r_{b \rightarrow u}^{\text{sl}}$, fitting procedure and imperfect detector simulation are combined in the systematic error. The uncertainties due to inaccurate simulation of tracking, particle identification, and cluster finding are estimated by varying for each source the efficiency within the expected error and taking the maximum change in the branching fraction as the error. For each of these sources the effects on simulated $b \rightarrow u$ and $b \rightarrow c$ events are correlated, and the associated shifts are summed linearly. The net contributions from the three sources are then summed in quadrature.

The CKM matrix element $|V_{ub}|$ is obtained directly from the partial branching fraction using $|V_{ub}|^2 = \Delta\mathcal{B}(B \rightarrow X_u \ell \nu)/(R \cdot \tau_B)$, where $\tau_B = (1.604 \pm 0.011) \text{ ps}$ is the average B lifetime [19]. R is the theoretical prediction of the partial rate $\Delta\Gamma(X_u \ell \nu)$ divided by $|V_{ub}|^2$. It is calculated for a given signal region and with a prompt lepton with $p_\ell^* \geq 1 \text{ GeV}/c$, by using an inclusive $B \rightarrow X_u \ell \nu$ decay generator [15] based on the latest theoretical studies [2, 3]. The values of R (in ps^{-1}) are $21.6 \pm 4.0(\text{SF})^{+2.4}_{-2.3}(\text{th.})$, $40.9 \pm 7.5(\text{SF})^{+3.2}_{-2.9}(\text{th.})$ and $33.2 \pm 6.8(\text{SF})^{+2.3}_{-2.3}(\text{th.})$ for the M_X/q^2 , M_X and P_+ signal regions, respectively. The R values and their errors (SF) are calculated using the shape function scheme [15] parameters $m_b(\text{SF}) = 4.52 \pm 0.07 \text{ GeV}/c^2$ and $\mu_\pi^2(\text{SF}) = 0.27 \pm 0.13 \text{ GeV}^2/c^2$ and their correlation, obtained by repeating the analysis from Ref. [20] with the predicted shapes of the $B \rightarrow X_s \gamma$ photon energy distributions from Ref. [15]. The theoretical error on R (th.) is estimated by varying the subleading shape functions (four models), the matching scales μ_h , μ_i , $\bar{\mu}$ and weak annihilation [15]. The values of $|V_{ub}|$ with errors are given in Table III. The total error on $|V_{ub}|$ is 13%, 12% and 14% for M_X/q^2 , M_X and P_+ regions, respectively. When the shape function parameters and R are better determined, $|V_{ub}|$ can be recalculated from $\Delta\mathcal{B}(B \rightarrow X_u \ell \nu)$ shown in Table II.

The precision of the $|V_{ub}|$ determination is better than previous measurements [4, 5, 21], due to the use of both a larger data sample and improved theoretical predictions [2, 3]. The effectiveness of $|V_{ub}|$ measurements using full reconstruction tagging is clear (Figs. 2(b), 3(a) and 3(b)). This is the first result to use the variable P_+ to select the $b \rightarrow u$ signal region and demonstrates that this method is competitive. Improvements in $|V_{ub}|$ deter-

minations using the P_+ method will be more significant with better shape function determinations in the future.

We thank the KEKB group for excellent accelerator operations, the KEK cryogenics group for efficient operation of the solenoid, and the KEK computer group and NII for valuable computing and Super-SINET network support. We acknowledge support from MEXT and JSPS (Japan); ARC and DEST (Australia); NSFC (contract No. 10175071, China); DST (India); the BK21 program of MOEHRD and the CHEP SRC program of KOSEF (Korea); KBN (contract No. 2P03B 01324, Poland); MIST (Russia); MHEST (Slovenia); SNSF (Switzerland); NSC and MOE (Taiwan); and DOE (USA).

We are grateful to B. Lange, M. Neubert and G. Paz for providing us with their theoretical computations implemented in an inclusive generator. We would specially like to thank M. Neubert for valuable discussions and suggestions.

- [1] C. W. Bauer, Z. Ligeti and M. Luke, Phys. Rev. **D 64**, 113004 (2001).
- [2] S. W. Bosch, B. O. Lange, M. Neubert and G. Paz, Phys Rev Lett. **93**, 221801(2004); Nucl. Phys. B **699**, 335 (2004).
- [3] M. Neubert, Eur. Phys. J. C **40**, 165 (2005); Phys. Lett. B **612**, 13 (2005); hep-ph/0411027; S. W. Bosch, M. Neubert and G. Paz, JHEP **0411**, 073 (2004).
- [4] B. Aubert *et al.* (BaBar Collaboration), Phys. Rev. Lett. **92**, 071802 (2004).
- [5] H. Kakuno *et al.* (Belle Collaboration), Phys. Rev. Lett. **92**, 101801 (2004).
- [6] A. Abashian *et al.* (Belle Collaboration), Nucl. Instrum. and Meth. A **479**, 117 (2002).
- [7] S. Kurokawa and E. Kikutani, Nucl. Instrum. and Meth. A **499**, 1 (2003), and other papers in this Volume.
- [8] R. Brun, F. Bruyant, M. Maire, A. C. McPherson and P. Zanarini, CERN Report No. DD/EE/84-1 (1984).
- [9] D. J. Lange, Nucl. Instrum. Meth. A **462**, 152(2001).
- [10] P. Ball, arXiv:hep-ph/0306251.
- [11] D. Scora and N. Isgur, Phys. Rev. D **52**, 2783 (1995).
- [12] F. De Fazio and M. Neubert, JHEP **9906**, 017 (1999).
- [13] QQ event generator, developed by CLEO Collaboration, see <http://www.lns.cornell.edu/public/CLEO/soft/QQ>.
- [14] M. Neubert, Phys. Rept. **245**, 259 (1994).
- [15] B. O. Lange, M. Neubert and G. Paz, hep-ph/0504071 and private communication with M. Neubert.
- [16] G. C. Fox and S. Wolfram, Phys. Rev. Lett. **41**, 1581 (1978).
- [17] H. Albrecht *et al.* (ARGUS Collaboration), Z. Phys. C **48**, 543 (1990).
- [18] J. E. Gaiser *et al.*, Phys. Rev. D **34**, 711 (1986).
- [19] S. Eidelman *et al.*, Phys. Lett. B **592**, 1 (2004).
- [20] A. Limosani and T. Nozaki (Heavy Flavor Averaging Group), hep-ex/0407052.
- [21] R. Barate *et al.* (ALEPH Collaboration), Eur. Phys. J. C **6**, 555 (1999); M. Acciarri *et al.* (L3 Collaboration), Phys. Lett. B **436** 174 (1998); P. Abreu *et al.* (DELPHI Collaboration), Phys. Lett. B **478** 14 (2000); G. Abbi-

endi *et al.* (OPAL Collaboration), Eur. Phys. J. C **21**, 399 (2001); A. Bornheim *et al.* (CLEO Collaboration),

CLEO-CONF 02-08.